

“Real-time” millikelvin thermometry in a semiconductor-qubit architecture

V. Champain ^{1,*} V. Schmitt ¹ B. Bertrand ² H. Niebojewski,² R. Maurand ¹ X. Jehl ¹
C.B. Winkelmann ¹ S. De Franceschi ¹ and B. Brun ^{1,†}

¹ *Commissariat à l'énergie atomique et aux énergies alternatives (CEA), Grenoble INP, Interdisciplinary Research Institute of Grenoble (IRIG)—Quantum Photonics, Electronics, and Engineering Laboratory (Pheliqs), Université Grenoble Alpes, Grenoble, France*

² *CEA Laboratoire d'électronique des technologies de l'information (Leti), Université Grenoble Alpes, Minatec Campus, Grenoble, France*

 (Received 25 August 2023; revised 16 February 2024; accepted 17 May 2024; published 17 June 2024)

We report local time-resolved thermometry in a silicon-nanowire quantum dot device designed to host a linear array of spin qubits. Using two alternative measurement schemes based on rf reflectometry, we are able to probe either local electron or bosonic bath temperatures with microsecond time scale resolution and a noise-equivalent temperature of $3 \text{ mK}/\sqrt{\text{Hz}}$. Following the application of short microwave pulses, causing local periodic heating, time-dependent thermometry can track the dynamics of thermal excitation and relaxation, revealing clearly different characteristic time scales. This work opens important prospects to investigate the out-of-equilibrium thermal properties of semiconductor quantum electronic devices operating at very low temperature. In particular, it may provide a powerful handle to understand heating effects recently observed in semiconductor spin-qubit systems.

Motivation

There is unintentional local heating by the high-frequency signal used with spin qubits due to dissipation (Joule, dielectric)

These local temperature changes affect the spin qubits

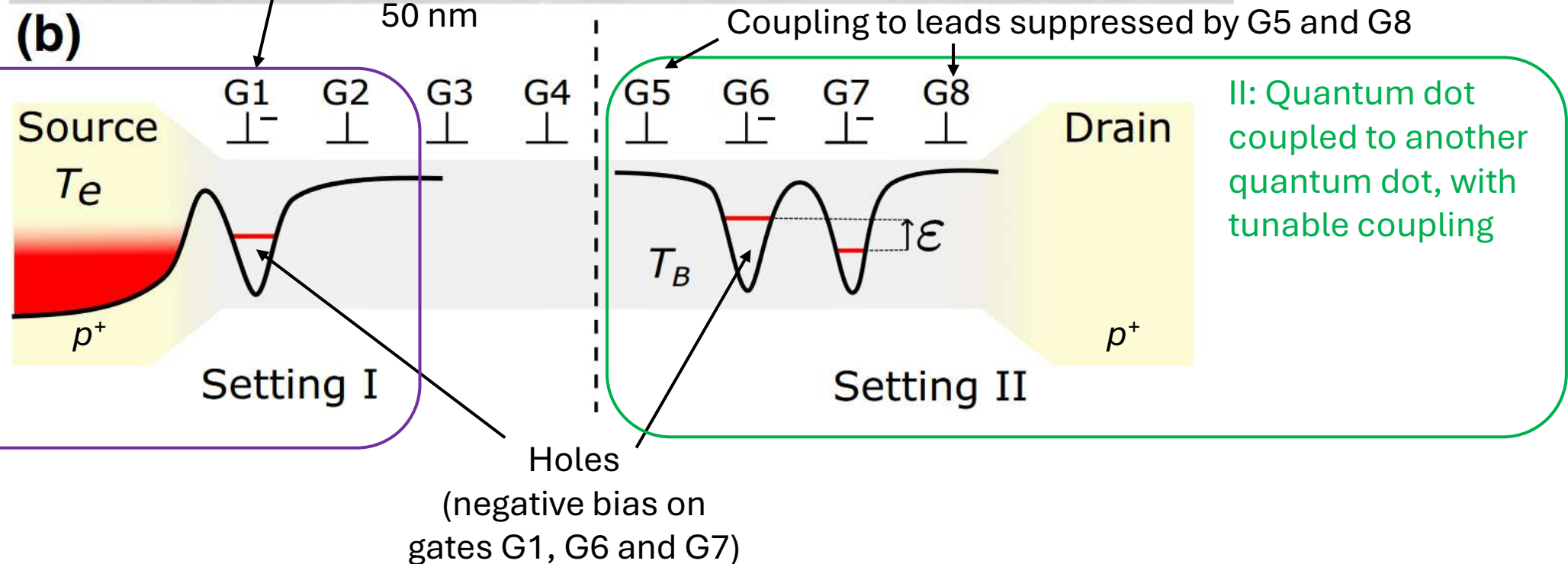
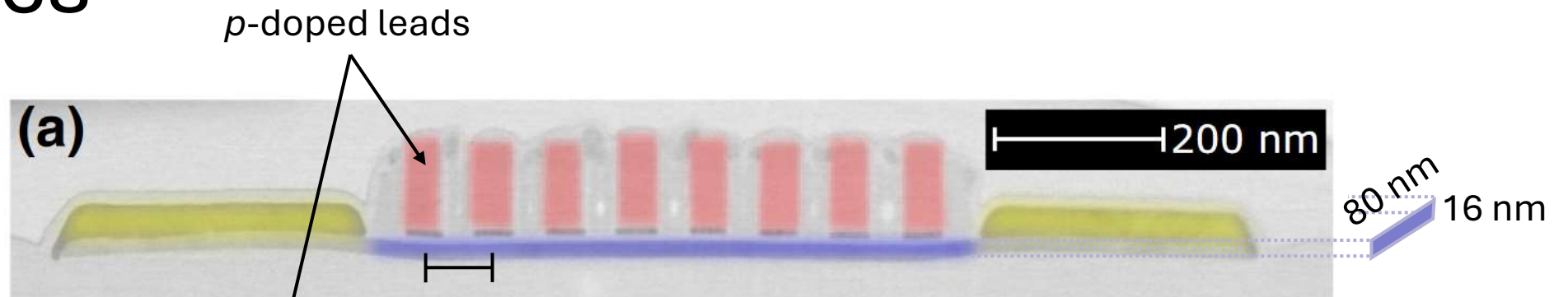
Temperature-dependence of spin qubit properties (Larmor frequency)

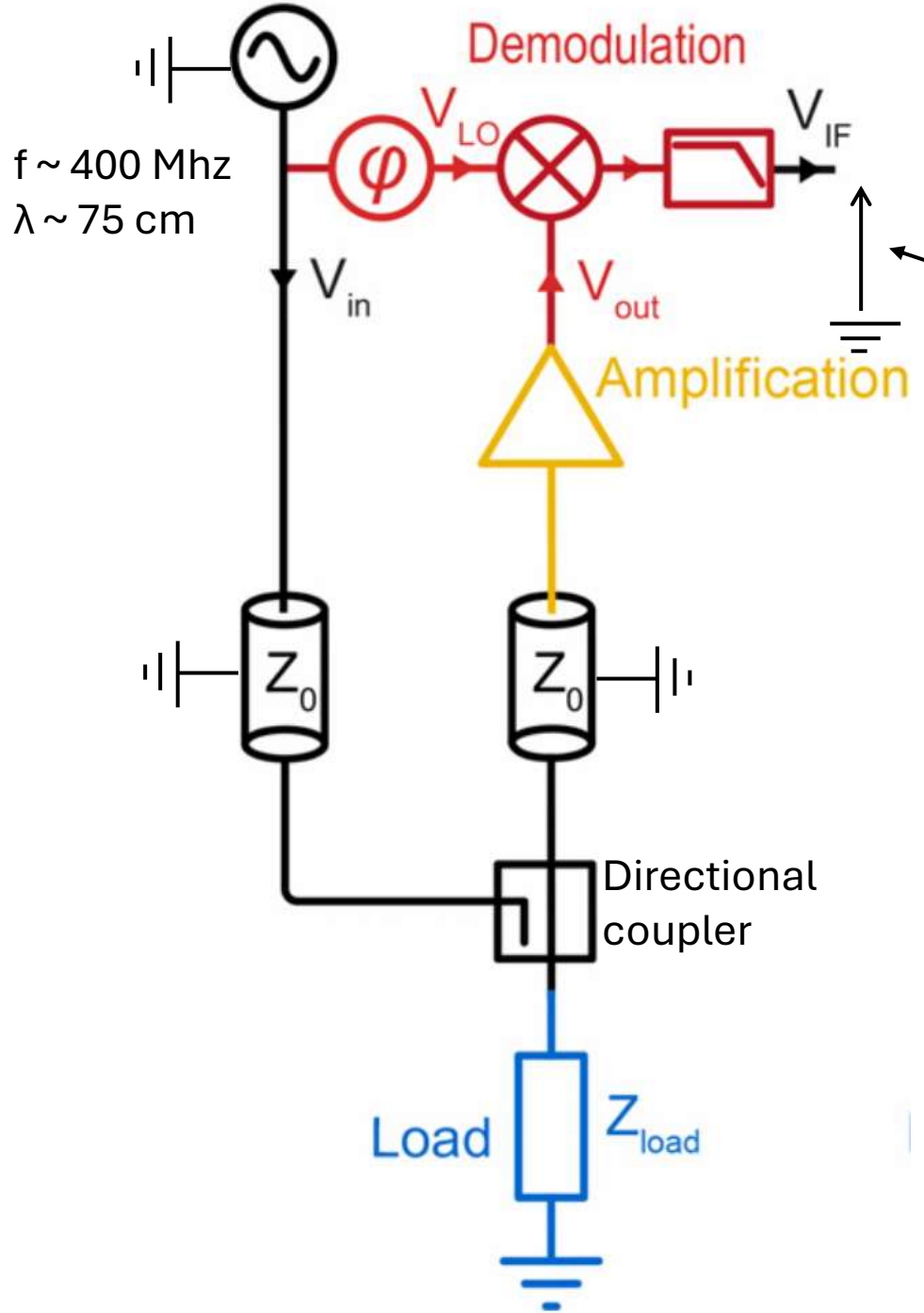
Spin decay and dephasing due to heating

Operating at higher overall temperature reduces the effect of this unintentional local heating, but sacrifices coherence

To improve qubits and have more qubits it is important to understand better these local heating effect

Devices





RF reflectometry

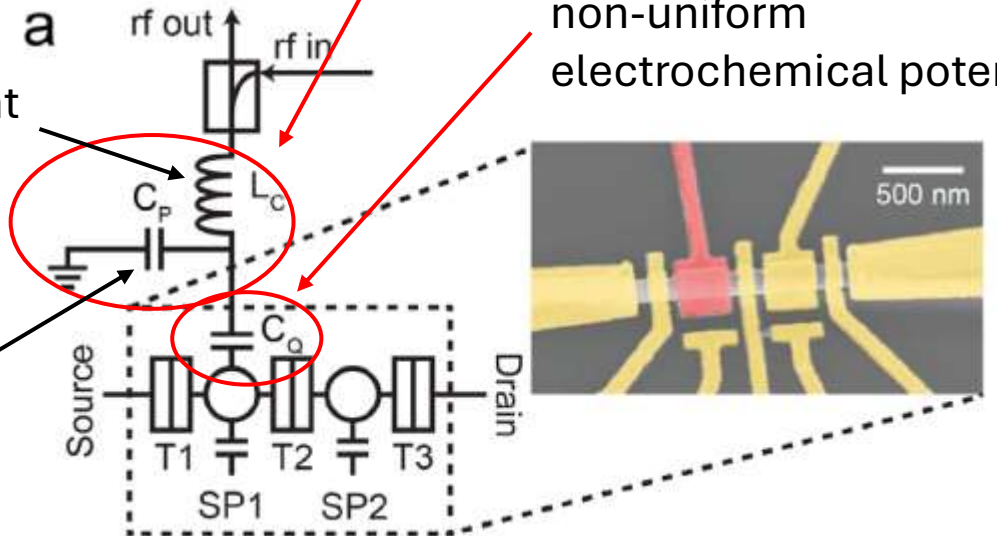
Reflected signal

LC resonator tank circuit

Additional “quantum” capacitance C_q due to non-uniform electrochemical potential

Surface-mount inductor

Parasitic capacitance



Adapted from Florian Vigneau *et al.*; Probing quantum devices with radio-frequency reflectometry. *Appl. Phys. Rev.* 1 June 2023; 10 (2): 021305. <https://doi.org/10.1063/5.0088229>

RF reflectometry with LC resonator

Fitting amplitude of reflected signal

$$S_{21,\text{dB}} = 20 \log \left| 1 + \frac{Q_i e^{i\varphi}}{Q_c \left[1 + 2iQ_i \left(\frac{f - f_r}{f_r} \right) \right]} \right|$$

At 52 mK:

$$Q_i = 385$$

$$Q_c = 62$$

$$Q = Q_i // Q_c = 53.4$$

$S_{21,\text{dB}}$ amplitude in dB of reflected signal

Q_i internal quality factor

Q_c external quality factor

Time resolution limit $\sim \tau = \frac{Q}{2\pi f_0} = 20 \text{ ns} @ f_0 = 400 \text{ MHz}$

Quantum capacitance, dot-lead situation

$$C_q(\varepsilon) = \alpha^2 e^2 [f * g](\alpha e \varepsilon)$$

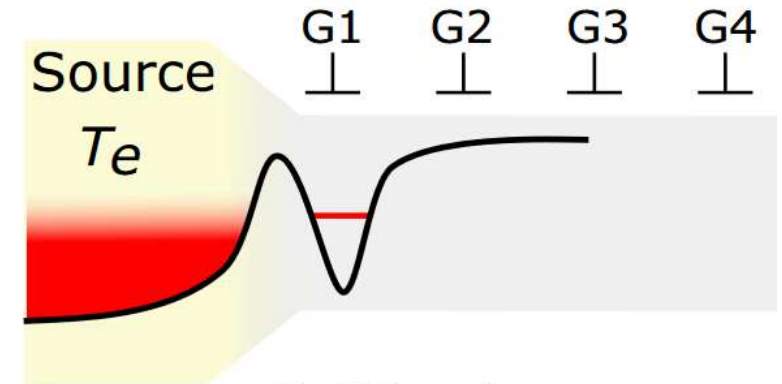
$$f(E) = \frac{1}{4k_B T_e} \cosh\left(\frac{E}{4k_B T_e}\right)^{-2}$$

Derivative of Fermi distribution in the lead broadened by $k_B T_e$

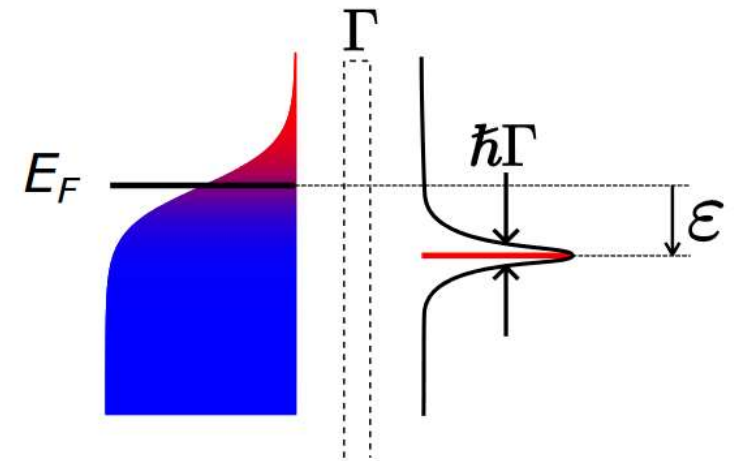
$$g(E) = \frac{\hbar \Gamma}{(\hbar \Gamma)^2 + E^2}$$

Dot density of states modeled by Lorentzian of width $\hbar \Gamma$

Regime: $\hbar \Gamma < k_B T_e$



Setting I



$$[f * g](x) = \int_{-\infty}^{+\infty} f(x - u) g(u) du \quad \text{“} = \int_{u+v=x} f(u) g(v) \text{”}$$

α gate lever-arm parameter

ε detuning in gate voltage

Γ tunnelling rate between dot and lead (angular frequency)

T_e electron temperature in the lead

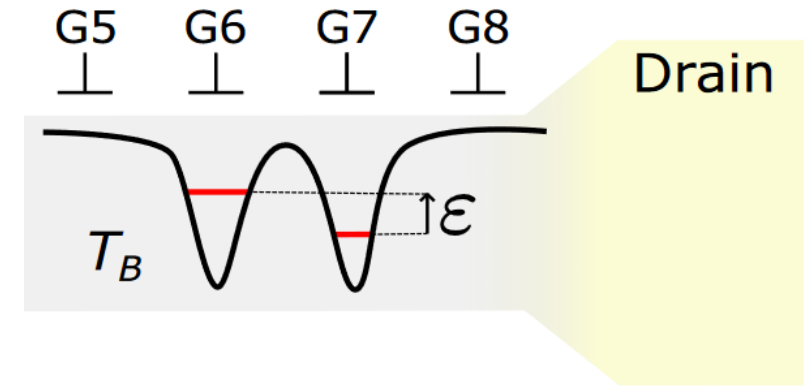
e electron charge

k_B Boltzmann constant

\hbar reduced Planck constant)

Quantum capacitance, double dot situation

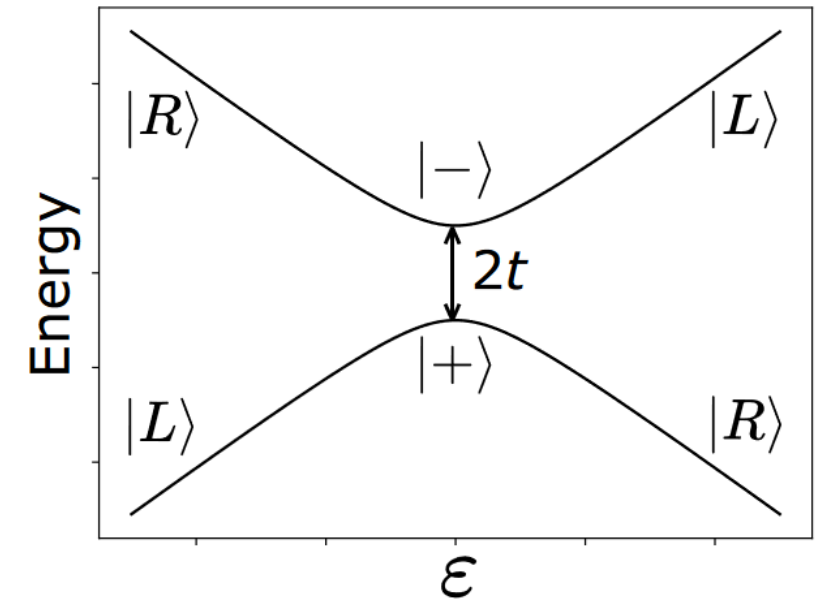
$$C_q(\varepsilon) = \alpha^2 e^2 \frac{2t^2}{((\alpha e\varepsilon)^2 + 4t^2)^{3/2}} \tanh\left(\frac{((\alpha e\varepsilon)^2 + 4t^2)^{1/2}}{2k_B T_B}\right)$$



where $k_B T_B = \frac{2t}{\ln\left(\frac{P_{|+\rangle}}{P_{|-\rangle}}\right)}$ Regime: $t \lesssim k_B T_B$

From Boltzmann distribution on two states

Setting II



α gate lever-arm parameter

ε detuning in gate voltage

t tunnel coupling between the two dots (energy)

$P_{|+\rangle}$ and $P_{|-\rangle}$ populations of $|+\rangle$ or $|-\rangle$ states

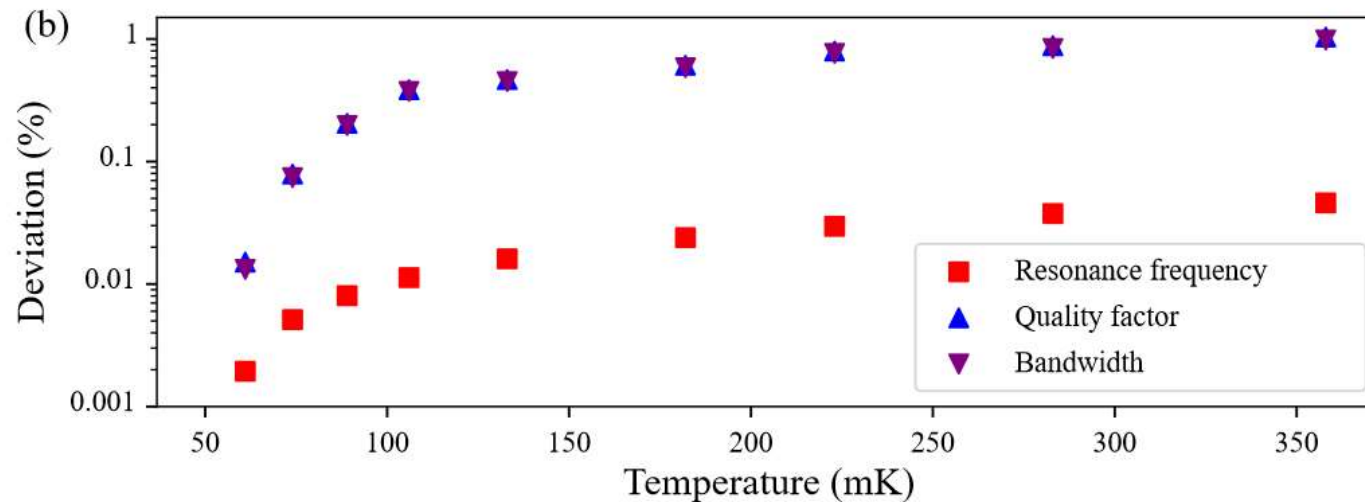
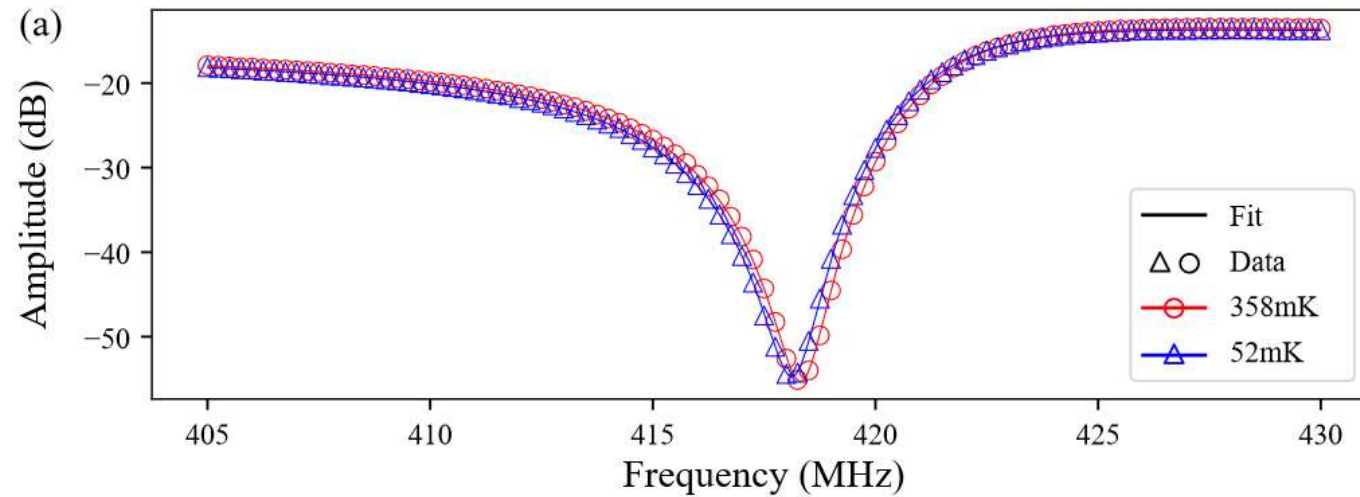
(hybridised (bonding and antibonding) states, at detuning $\varepsilon = 0$)

e electron charge

k_B Boltzmann constant

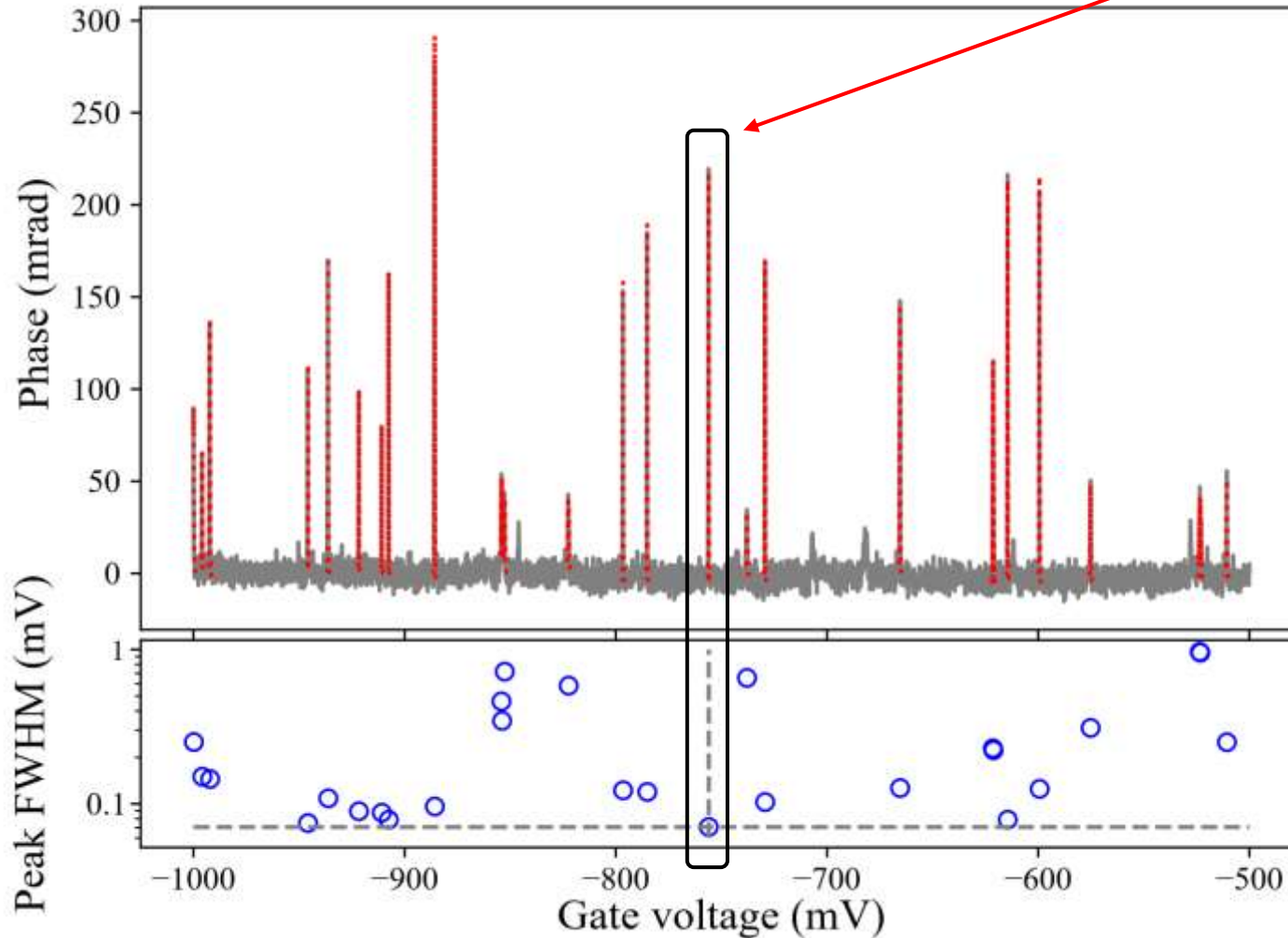
\hbar reduced Planck constant)

Preliminary checks and setup: LC resonator



Preliminary checks and setup: dot-lead transition selection (setting I)

Narrowest peak: lowest tunnelling rate Γ , quantum capacitance most sensitive to temperature in lead



$$\Gamma/2\pi = 383 \pm 38 \text{ MHz}$$

Preliminary checks and setup: temperature sensitive regime for **double quantum dot**, with low tunnel coupling (setting II)

$$t/h = 2.03 \pm 0.04 \text{ GHz}$$

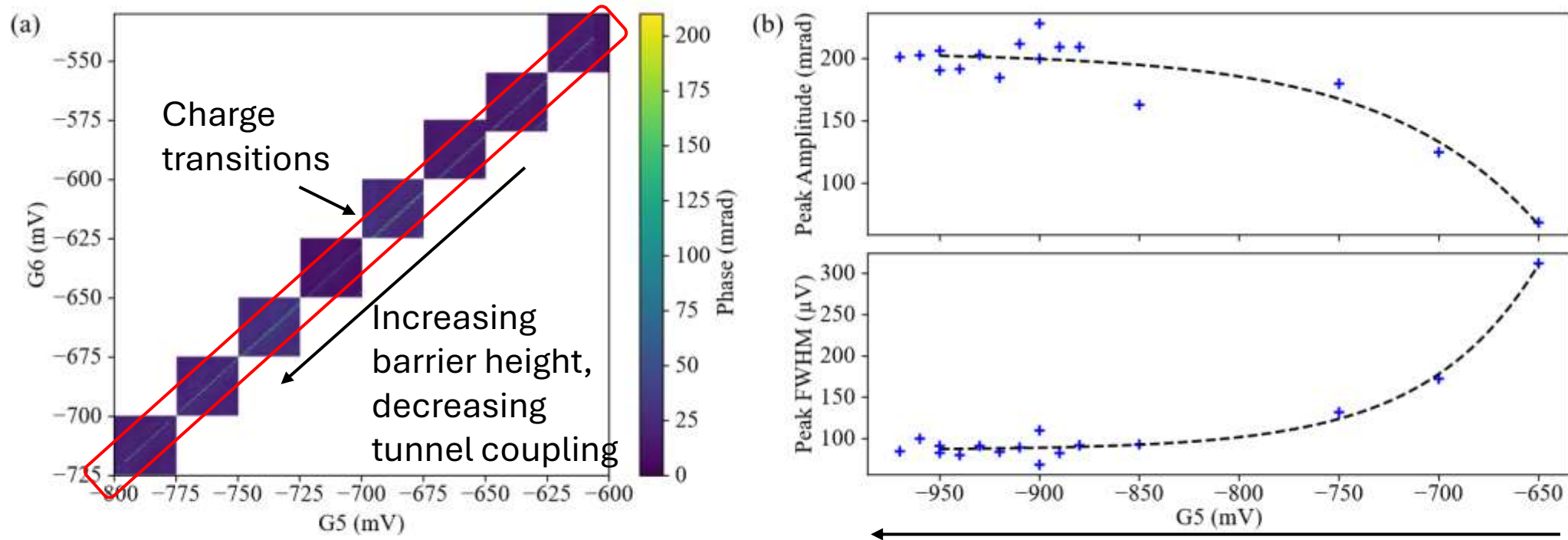
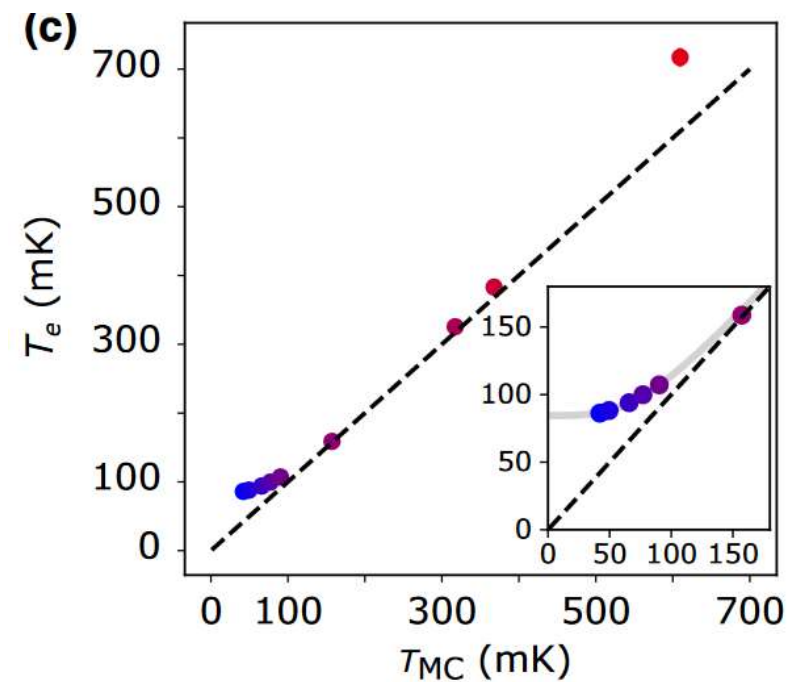
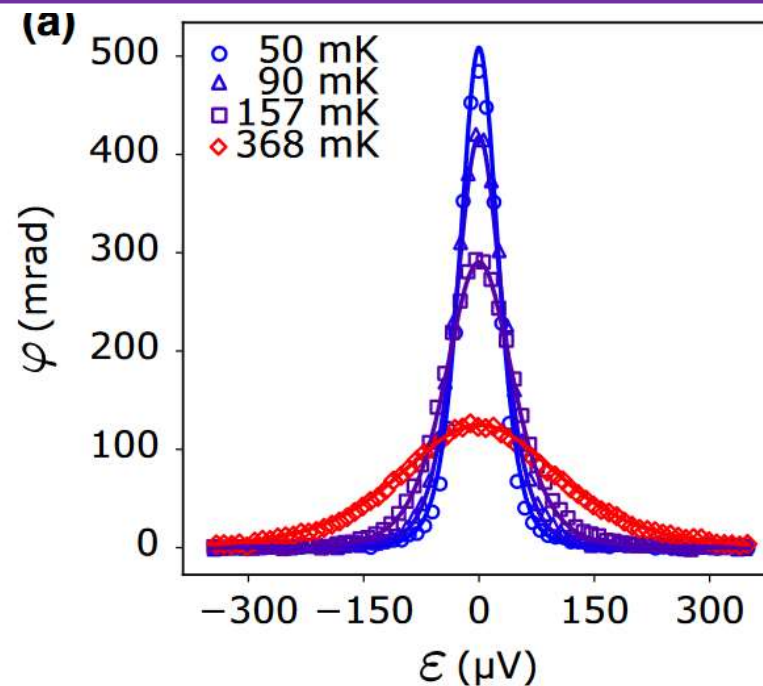


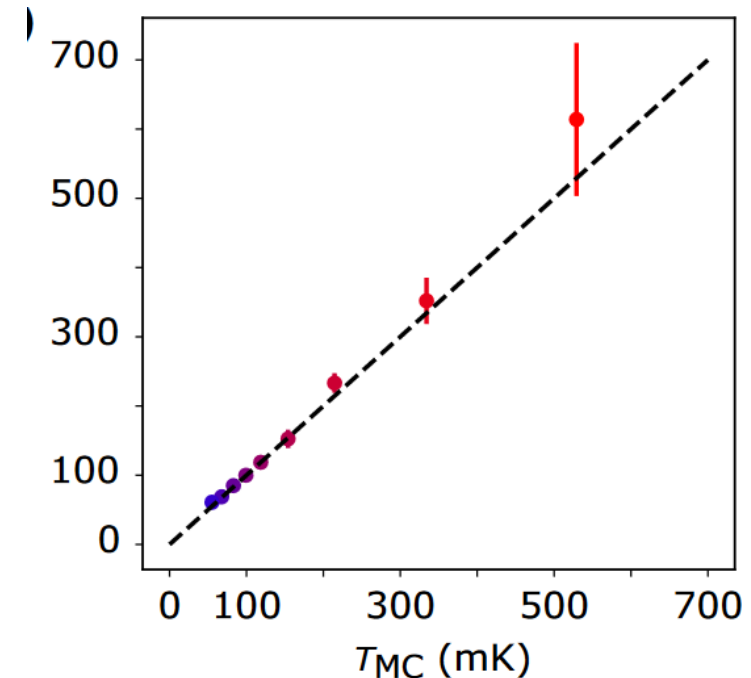
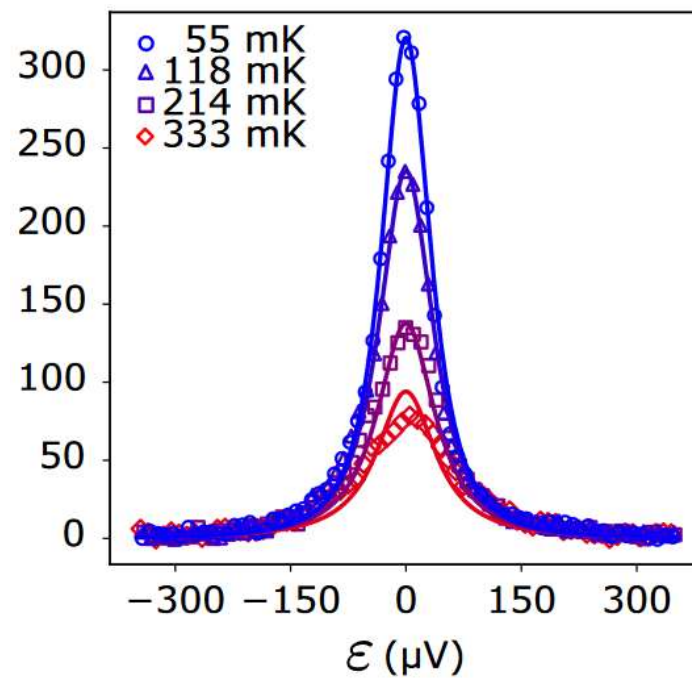
FIG. S3. **Isolated double dot charge stability diagram.** (a) Charge stability diagram showing 'infinite' interdot transitions. (b) Peak amplitude and width as a function of the gate voltage, showing a way to reduce the tunnel coupling.

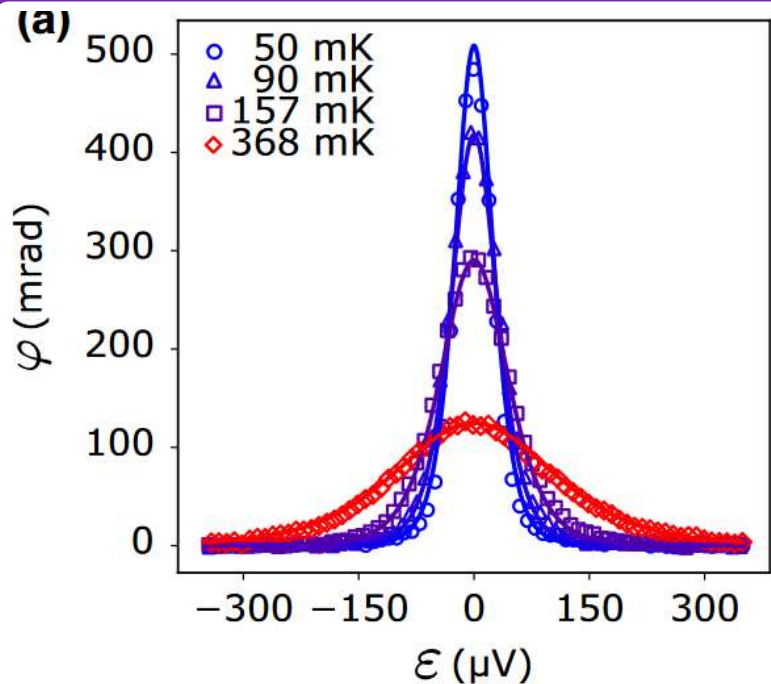
Results

I: Quantum dot
coupled to lead
(thermal bath)

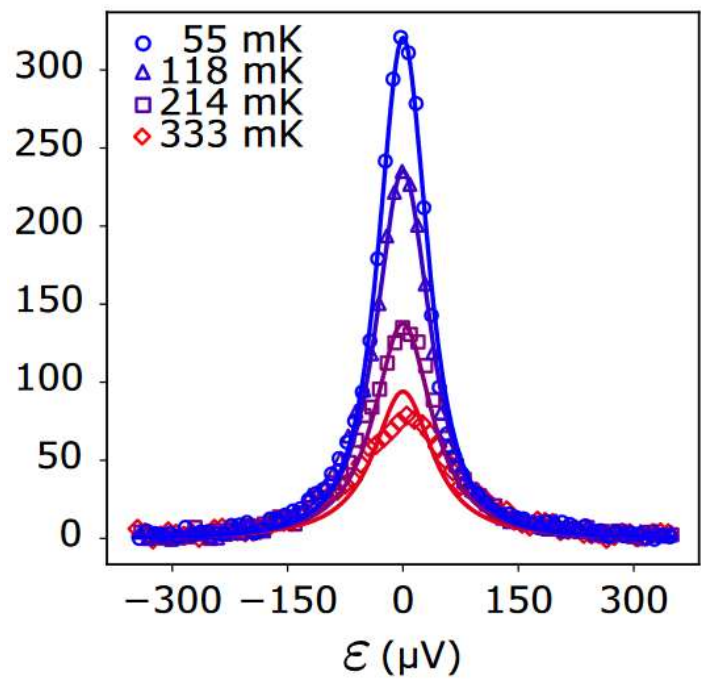
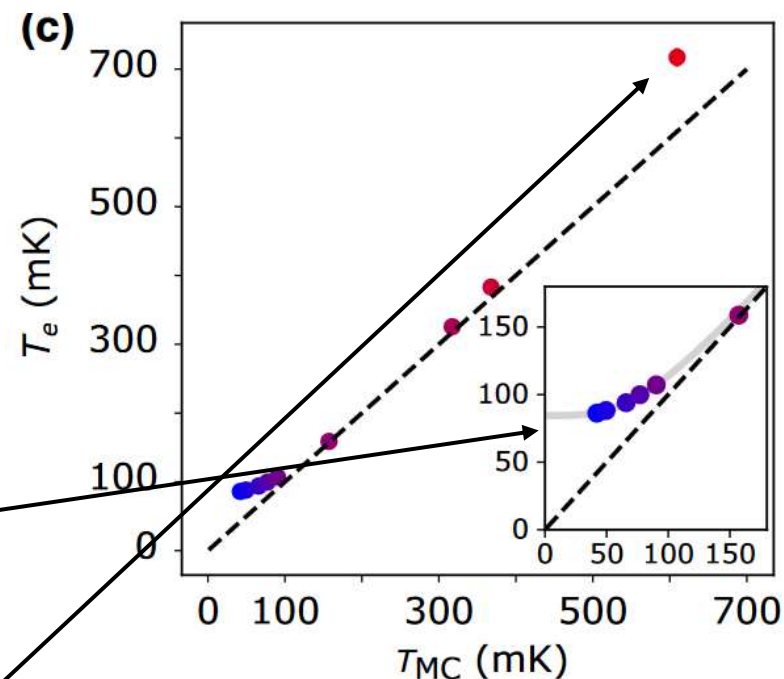


II: Quantum dot
coupled to another
quantum dot, with
tunable coupling

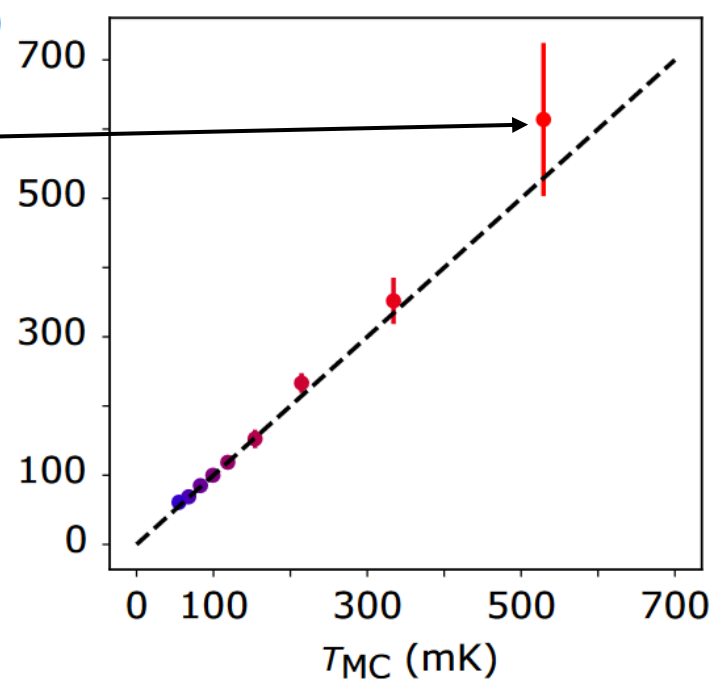




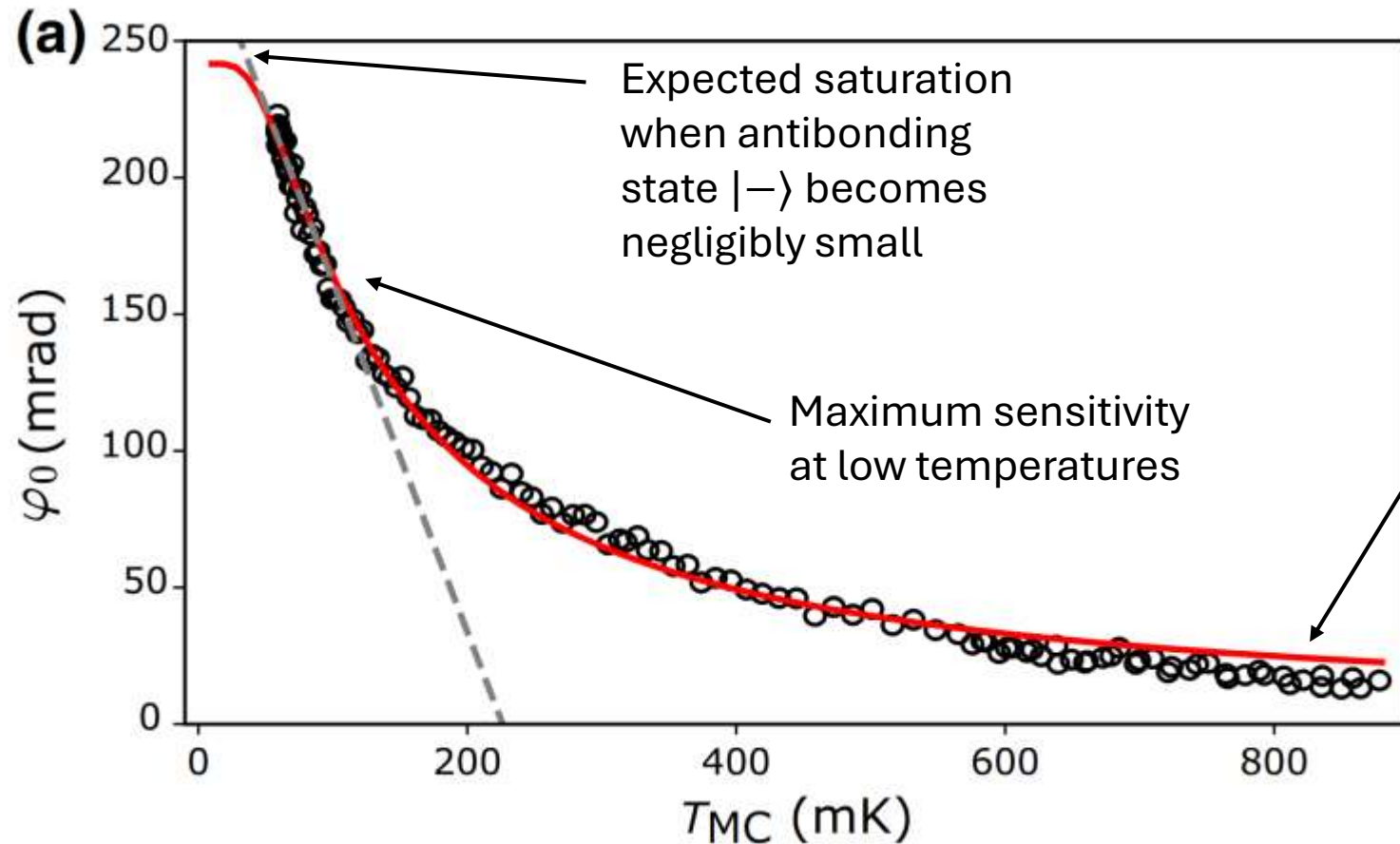
Fitting $T_e = (T_{\text{MC}}^n + T_0^n)^{1/n}$
 $T_0 = 84$ mK and $n = 3.4 \neq 5$



Higher energy
 quantum dot
 levels not
 accounted for
 in model



Calibration of double quantum dot thermometer: reflected signal phase at zero detuning ($\varepsilon = 0$)



Function fitted in red:

$$\varphi_0 = \kappa \times \frac{1}{2t} \tanh\left(\frac{t}{k_B T_{MC}}\right)$$

(from quantum capacitance formula at $\varepsilon = 0$ and $T_B = T_{MC}$)

$$t/h = 1.72 \pm 0.04 \text{ GHz}$$

(In principle not needed: Landau-Zener-Stückelberg interference)

Noise-equivalent temperature

Expression of noise-equivalent temperature:

$$\text{NET} = \frac{S_{\varphi\varphi}}{\left| \frac{\partial\varphi_0}{\partial T_{\text{MC}}} \right|}$$

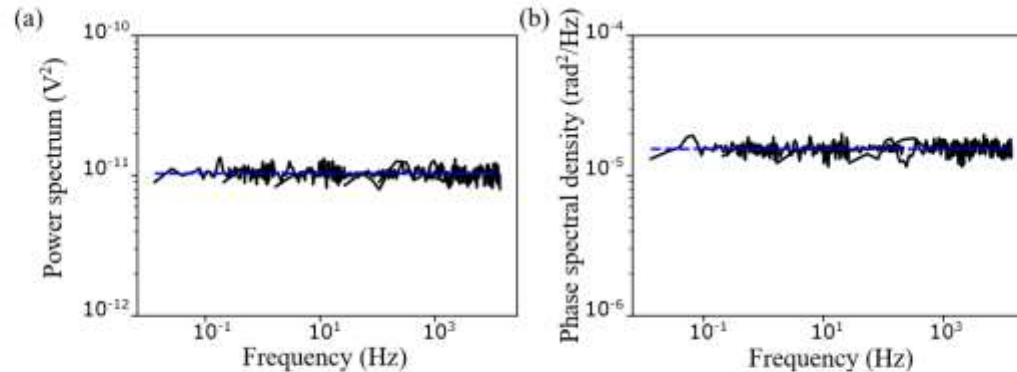


FIG. S4. **Noise spectrum.** a) Power spectrum computed using Welch's method⁹, showing a white noise spectrum with a noise floor $S_P = 1.03 \pm 0.09 \times 10^{-11} \text{V}^2$. b) Phase spectral density, showing a white noise spectrum with a noise floor $S_{\varphi\varphi} = 3.9 \pm 0.2 \text{ mrad}/\sqrt{\text{Hz}}$

$S_{\varphi\varphi} = 3.9 \pm 0.2 \text{ mrad}/\sqrt{\text{Hz}}$ is the phase-noise amplitude

In the region of maximum sensitivity (temperature close to base temperature $\sim 55 \text{ mK}$)

$$\text{NET} = 3.0 \pm 0.2 \text{ mK}/\sqrt{\text{Hz}}$$

(with $\left| \frac{\partial\varphi_0}{\partial T_{\text{MC}}} \right| = 1.28 \text{ mrad}/\text{mK}$ fitted in previous plot)

Could be improved with better impedance matching

Noise-equivalent temperature

Starting from the expression of reflected signal phase at zero detuning fitted previously

$$\varphi_0 = \kappa \times \frac{1}{2t} \tanh\left(\frac{t}{k_B T_{MC}}\right)$$

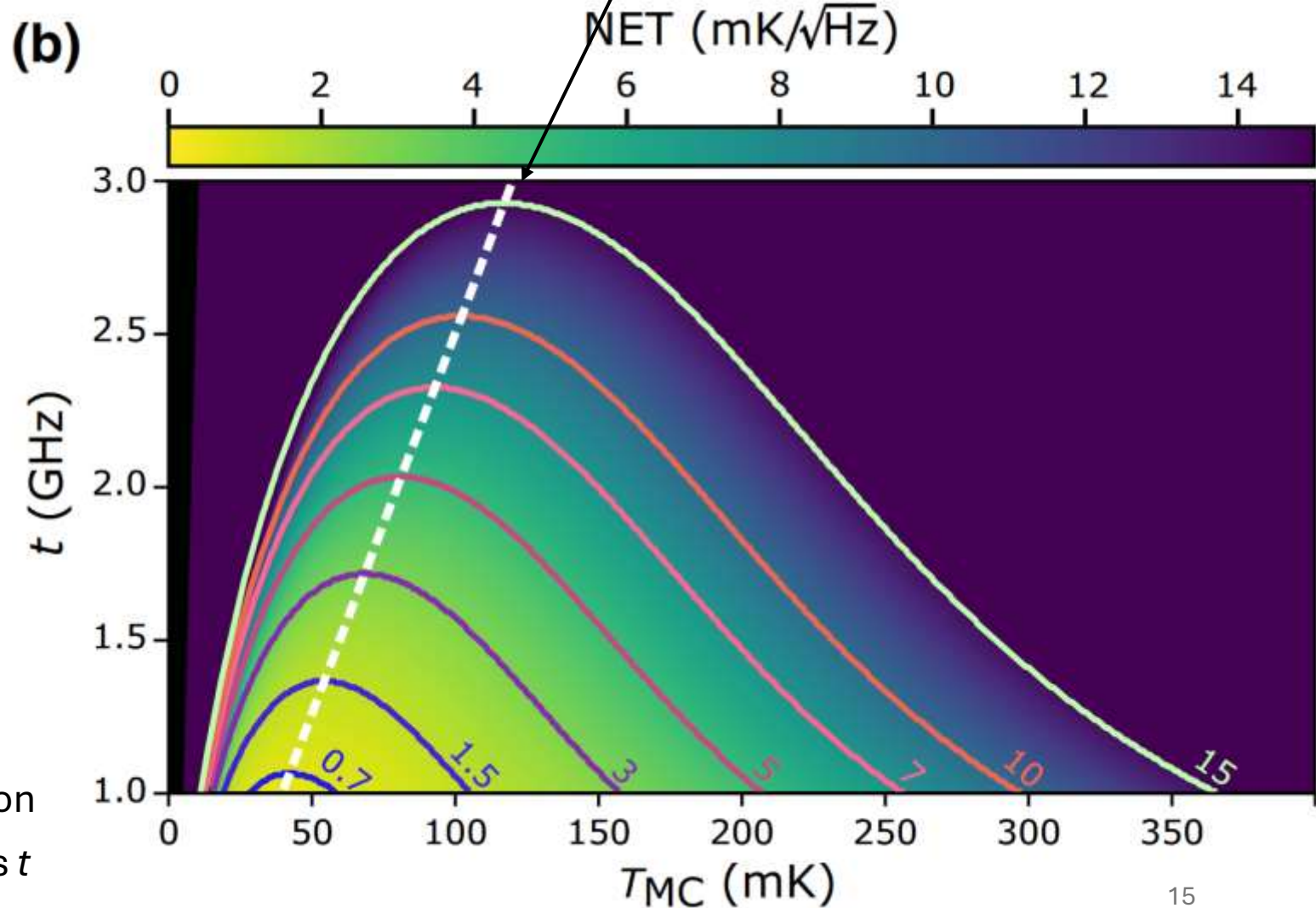
Assuming dispersive coupling between the LC resonator and the isolated double quantum dot implies:

$$\kappa = A_0 \left(\frac{1}{2t + f_r} + \frac{1}{2t - f_r} \right)$$

Resonance frequency of "tank" circuit

Now t is used as parameter and the expression the NET = $\frac{S_{\varphi\varphi}}{\left| \frac{\partial \varphi_0}{\partial T_{MC}} \right|}$ can be calculated at various t

Optimal tunnel coupling depending on temperature



“Real-time” thermometry (proof of concept)

- Noise-equivalent temperature is too large to resolve temperature fluctuations at microsecond scale
- But noise can be reduced with averaging if heating event is periodic or deterministic/reproducible
- For example, microwave bursts used for operation of spin-qubit devices

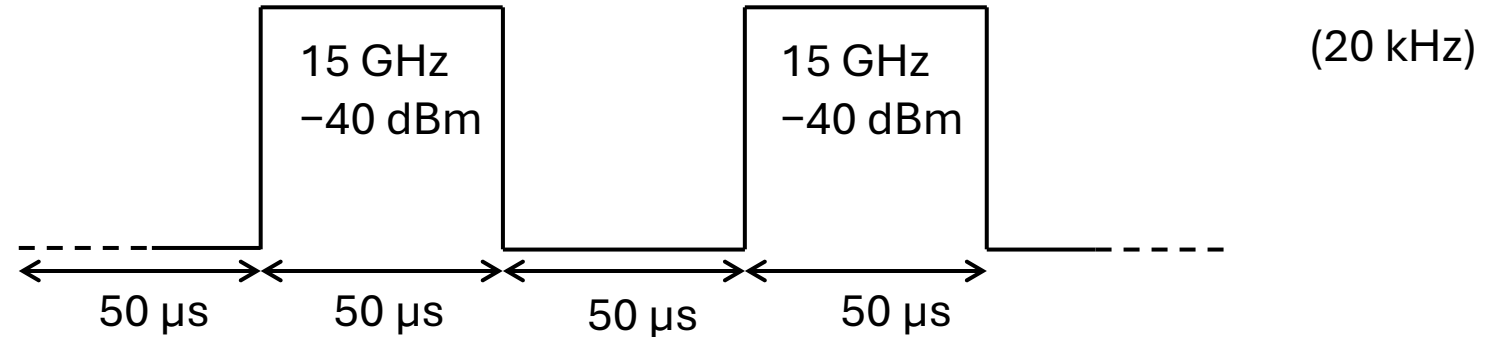
Limiting bandwidths

- Response time of measurement apparatus (~ 20 ns)
- Charge relaxation time T_1 toward a thermal state (~ 15 ns)

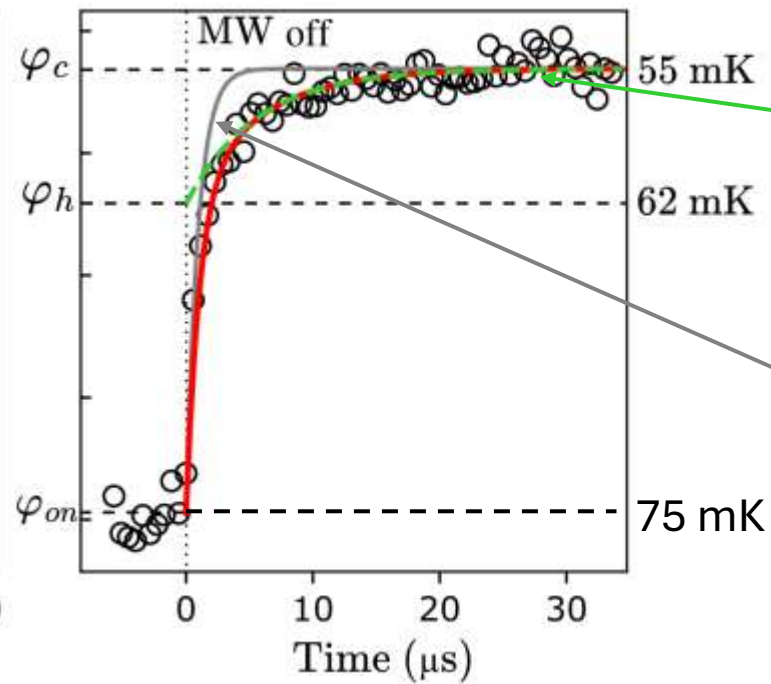
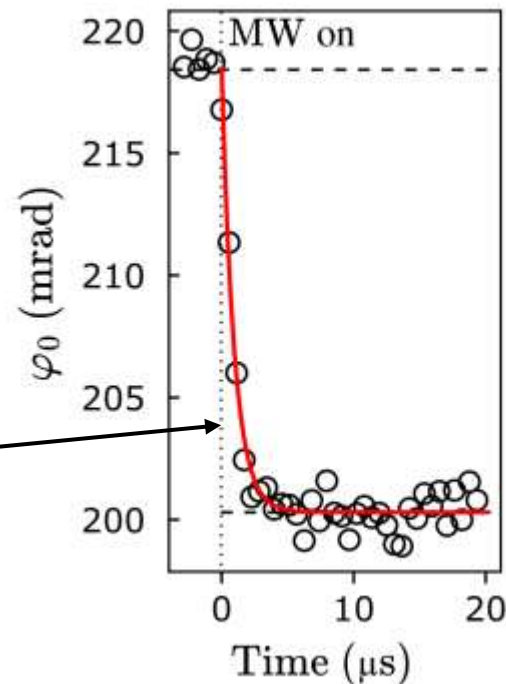
Hence few MHz resolution

Proof of concept: periodic microwave burst on nearby gate

Lockin parameters:
1.7 MHz
400 ns integration window



Exponential decay
 $\tau = 0.93 \pm 0.35 \mu$ s
(too short)



Slow exponential decay ($\tau = 67.0 \pm 1.5 \mu$ s): relaxation of the heat bath?

Fast exponential decay: T1 relaxation?

Conclusion and outlook

- “Noninvasive, nongalvanic thermometers”
- Both Fermi reservoir (**dot-lead setting**) and local bosonic temperature in semiconductor quantum dot (**double quantum dot setting**)
- State-of-the-art noise-equivalent temperature of $3 \text{ mK}/\sqrt{\text{Hz}}$
- Temperature variations measured on microsecond scale when averaging is possible
- Technique demonstrated in silicon MOS device, could be applied on other platforms: Si-Ge-based heterostructures?

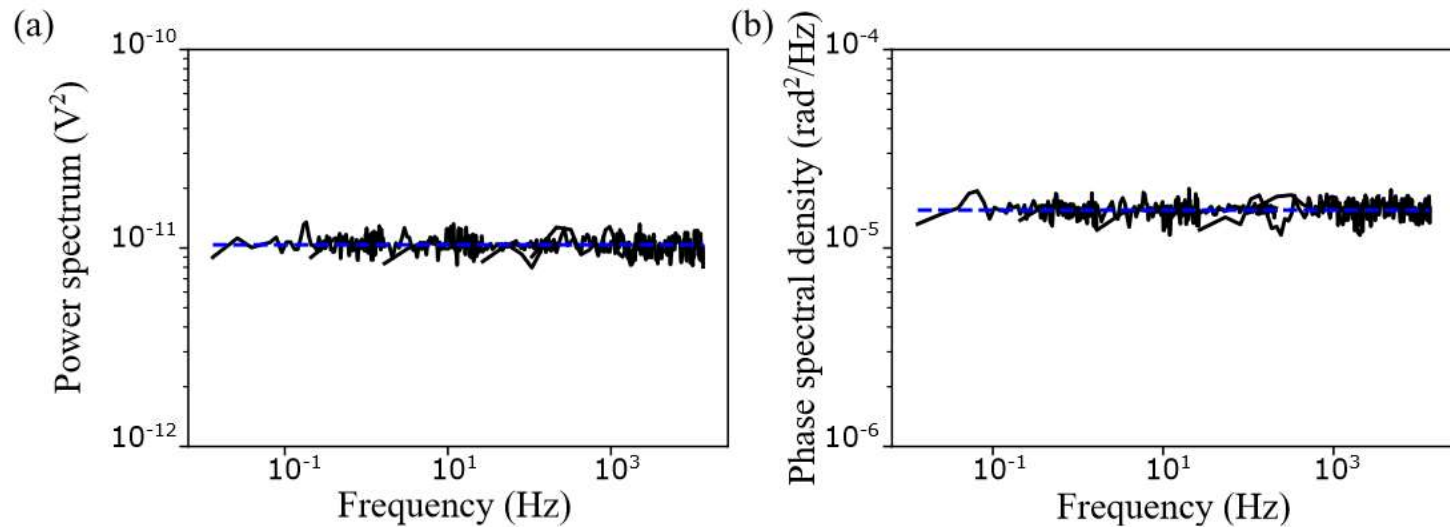


FIG. S4. **Noise spectrum.** **a)** Power spectrum computed using Welch's method⁹, showing a white noise spectrum with a noise floor $S_P = 1.03 \pm 0.09 \times 10^{-11} \text{V}^2$. **b)** Phase spectral density, showing a white noise spectrum with a noise floor $S_{\varphi\varphi} = 3.9 \pm 0.2 \text{ mrad}/\sqrt{\text{Hz}}$

The two quadratures of the demodulator I and Q are measured for different sampling frequencies to access noise spectrum in a wide frequency range. From the noise floor we can access to the noise temperature NT :

$$NT = \frac{S_P}{10^{\frac{G_{dB}}{10}} B \times 4k_B R} \quad (\text{S16})$$

Where S_P is the noise floor, G_{dB} is the gain in dB of the room temperature amplifier, B is the bandwidth of the demodulator and R is the 50Ω -impedance of the transmission line. We find a $NT = 1.9 \pm 0.3 \text{ K}$, where as the cryogenic amplifier (LNF-LNC 0.2-3 A s/n 1410Z) used in this experiment has a noise temperature of around 2 K